# Synthesis of a Novel Star Polymer Consisting of a Dendritic Polyamidoamine Core and Polystyrene Arms and Its Self-Assembly To Form Large Multimolecular Micelles

**Yili Zhao,[1] Yantao Song,[1] Wei Jiang,[1] Bao Zhang,[1] Yapeng Li,[1] Ke Sha,[1] Shuwei Wang,[1] Liang Chen,[2] Lina Ma,[3] Jingyuan Wang[1]**

[1]*Alan G. MacDiarmid Institute, Jilin University, Changchun 130023, People's Republic of China*
[2]*First Hospital, Jilin University, Changchun 130021, People's Republic of China*
[3]*Department of Bioengineering, College of Pharmacy, Jilin University, Changchun 130021, People's Republic of China*

Received 25 July 2007; accepted 25 January 2008
DOI 10.1002/app.28092
Published online 11 April 2008 in Wiley InterScience (www.interscience.wiley.com).

**ABSTRACT:** This work is focused on the synthesis and self-assembly of novel dendritic star polymers with a dendritic polyamidoamine core and many linear polystyrene arms. The polymers can synchronously form unimolecular micelles (ca. 10 nm) and large multimolecular micelles (ca. 100 nm) in selected solvents (tetrahydrofuran/methanol) at room temperature. Atomic force microscopy, scanning electron microscopy, and dynamic light scattering measurements have provided direct evidence that the large micelles are a kind of multimicelle aggregate with the basic building units of unimolecular micelles. Accordingly, a possible self-assembly process is put forward, and a new aggregate model, termed *multimicelle aggregate*, is suggested to explain the formation of the large micelles. In the multimicelle aggregate model, the large micelles are the aggregates of small micelles associated by intermicellar interactions such as hydrogen bonds and p–p stacking interactions. It is the first demonstration of the self-assembly mechanism for the large multimolecular micelles generated from the solution self-assembly of dendritic star polymers. © 2008 Wiley Periodicals, Inc. J Appl Polym Sci 109: 1039–1047, 2008

**Key words:** atom transfer radical polymerization (ATRP); micelles; self-assembly; star polymers

## INTRODUCTION

In recent years, star homopolymers and star block copolymers have attracted considerable attention because of their particular bulk and solution properties.[1–3] Two general synthetic methods have been developed to prepare star polymers. One is the so-called arm-first method, in which reactive linear polymers are coupled with a multifunctional reagent.[4–10] The other is the so-called core-first method, in which a multifunctional initiator is used to initiate the polymerization of a monomer to form a multiarm star polymer.[11–13] Dendrimers and hyperbranched polymers, with numerous functional groups, have been used as core moieties for the preparation of star polymers.[14–19]

Currently, molecular self-assembly is always an active topic of research because it produces a variety of nanoobjects with various beautiful shapes[20] that have potential technological applications in many research fields such as medicine, biochemistry, and material science.[21] Molecular self-assembly of amphiphilic block copolymers has generated many impressive aggregates with various morphologies such as micelles, vesicles, tubes, rods, and lamellae.[22–27] Among them, micelles are the most commonly and widely reported supramolecular aggregates.

Generally, micelles can be classified as simple micelles and complex micelles according to their structure and size. The simple micelle was called a primary micelle by Eisenberg and coworkers;[28,29] it is about two molecules in diameter and often smaller than 50 nm. It is formed by the primary aggregation of block copolymers due to microphase separation in a selective solvent and has an aggregated structure. The complex micelle is more complicated in its structure and larger in size (often >100 nm) and has attracted lots of attention from both academia and industry. Eisenberg and coworkers[30,31] pointed out that these complex micelles are ''large compound micelles'' formed by the secondary aggregation of primary micelles or reverse micelles.

In this work, we report on the synthesis of a novel dendritic star polymer, polyamidoamine-*graft*-

*Correspondence to:* J. Wang (jingyuan@jlu.edu.cn).
Contract grant sponsor: Natural Science Foundation of China; contract grant number: 20574028.

**TABLE I**
**IR Spectroscopy Parameters of the PAMAM Dendrimers with Generations 0.5–2.0, PAMAM–OH with Generation 2, and PAMAM–Br with Generation 2**

| Sample | ν(−$CH_2$−) | δ(−$CH_2$−) | ν(C−N) | ν(C=O) | ν(C−O) | ν(CONH) | ν(−NH−) | ν(−OH) | ν(C−Br) |
|---|---|---|---|---|---|---|---|---|---|
| G0.5 | 2950 | 1440 | 1190 | 1730 | 1200 | | | | |
| | 2830 | | | | | | | | |
| G1.0 | 2940 | 1450 | 1130 | | | 1650 | 3280 | | |
| | 2860 | | | | | 1550 | 3070 | | |
| G1.5 | 2950 | 1440 | 1190 | 1740 | 1200 | | 3300 | | |
| | 2830 | | | | | | | | |
| G2.0 | 2940 | 1450 | 1130 | | | 1650 | 3280 | | |
| | 2860 | | | | | 1550 | 3070 | | |
| G2–OH[a] | 2930 | 1450 | 1250 | | | 1650 | 3280 | 3350 | |
| | 2850 | | | | | 1550 | 3070 | | |
| G2–Br[b] | 2910 | 1450 | 1250 | 1740 | 1200 | 1650 | 3430 | | 680 |
| | 2840 | | | | | 1550 | 3070 | | |

[a] G2–OH denotes modified PAMAM dendrimers with a peripheral hydroxyl.
[b] G2–Br denotes modified PAMAM dendrimers with a peripheral α-bromoester.

polystyrene (PAMAM-*g*-PSt), which is prepared by the core-first method via atom transfer radical polymerization (ATRP) of styrene (St) on the surface of a dendritic polyamidoamine (PAMAM) core. The self-assembly of large micelles from a series of newly synthesized dendritic star polymers has been found to lead to complex multimolecular micelles formed by the secondary aggregation of unimolecular micelles. The results indicate that the PAMAM-*g*-PSt molecules can aggregate into large spherical micelles (ca. 100 nm) with controlled sizes, and the micelle size increases as the molar ratio of St to the macroinitiator increases. To the best of our knowledge, this is the first demonstration of the aggregated structures inside the large micelles that self-assemble from dendritic star polymers.

## EXPERIMENTAL

### Materials

CuCl, purchased from Shanghai Chemical Co. (Shanghai, China; analytical reagent, 97.0%), was purified by stirring in acetic acid, filtered, washed with ethanol for the removal of $Cu^{2+}$, and then dried.[32] 1,1,4,7,10,10-Hexanemethyltriethylenetetramine (HMTETA; 98%) was purchased from Aldrich Chemical Co. and used as received. St (Beijing Chemical Co., Beijing, China; 98%) was extracted with a 5% solution of sodium hydroxide, stirred over calcium hydroxide for 24 h, distilled *in vacuo*, and stored at 5°C before use. Triethylamine (TEA; analytical reagent, 99.0%), ethylenediamine, and *N,N*-dimethylformamide (DMF) were dried with calcium hydroxide overnight and then distilled under reduced pressure before use.

### Synthesis of the PAMAM dendrimer macroinitiator

PAMAM dendrimers were synthesized with modifications first developed by Tomalia et al.[33] A typical experimental procedure is based on an ethylenediamine core, and branched units are constructed from both methyl acrylate and ethylenediamine. The detailed IR spectroscopy parameters of PAMAM are indicated in Table I. Then, PAMAM dendrimers are modified by two-step reactions to obtain bromine-terminated polyamidoamine (PAMAM–Br), which acts as a macroinitiator for ATRP. Scheme 1 outlines the chemical routes for two-step modifications of a functional PAMAM dendrimer with generation 2.

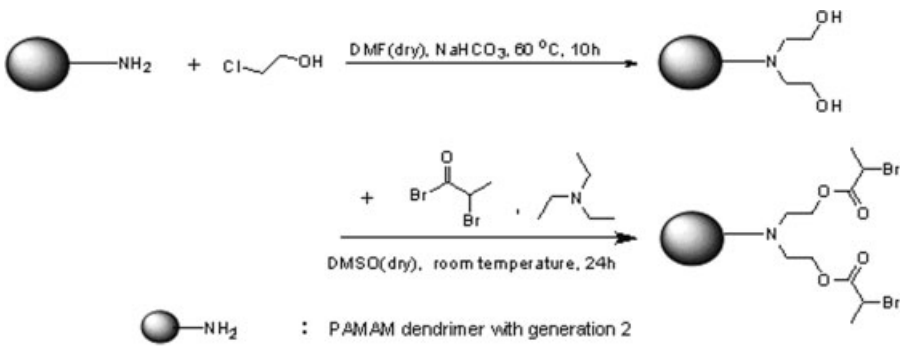


**Scheme 1** Synthesis of the PAMAM–Br macroinitiator.

### Synthesis of hydroxyl-terminated polyamidoamine (PAMAM–OH)

PAMAM–OH was prepared with a modified literature method.[34,35] Typically, in a three-necked, round-bottom flask equipped with a thermometer, dropping funnel, and magnetic stirrer, 4 g (0.0028 mol) of a PAMAM dendrimer of two generations was dissolved in 100 mL of DMF, and then 3.63 g (0.0448 mol) of chlorohydrin was added dropwise under vigorous stirring at room temperature for 30 min. The mixture solution was heated at 60°C for 10 h under vigorous stirring. At the same time, nitrogen gas was bubbled for the removal of the HCl byproduct. After the reaction was completed, the solvent was removed by vacuum distillation, and the residue was dried *in vacuo* at 40°C for 48 h.

IR (KBr): 3460–3278 (OH), 1646 (C=O), 1540 ($\delta_{NH}$ + $\nu_{C-N}$), 1238 (C—N), 2840 (s, $CH_2$), 2931 $cm^{-1}$ (as, $CH_2$). $^1$H-NMR ($D_2O$): δ(>N$CH_2CH_2$N<) = 2.16 ppm, δ(—$CH_2CH_2$N<) = 2.59–3.43 ppm, δ(—$CH_2CH_2$ CONH—) = 2.38 ppm, δ(—NH$CH_2CH_2$—) = 3.73 ppm, δ(>N$CH_2CH_2$OH) = 4.07 ppm.

### Synthesis of PAMAM–Br

In a three-necked, round-bottom flask equipped with a thermometer, dropping funnel, and magnetic stirrer, 4 g of PAMAM–OH with generation 2 was dissolved in 40 mL of dimethyl sulfoxide (DMSO), and then 6 mL of TEA was added under vigorous stirring at room temperature for 30 min. At the same time, 4 mL of 2-bromopropanoyl bromide was dissolved in 40 mL of DMSO under vigorous stirring at room temperature and then slowly dropped into the PAMAM–OH solution. The reaction was maintained at room temperature for 24 h. After the reaction was completed, the solvent and other volatile products were removed by distillation *in vacuo*. The obtained product was redissolved in methanol and precipitated from cold acetone as an oily, viscid lump, which was dried in a vacuum oven at room temperature for a week.

IR (KBr): 669 (C—Br), 1646 (C=O), 1540 ($\delta_{NH}$ + $\nu_{C-N}$), 1238 (C—N), 2840 (s, $CH_2$), 2931 (as, $CH_2$), 3433 $cm^{-1}$ (>NH). $^1$H-NMR ($D_2O$): δ(—CHBr$CH_3$) = 1.22 ppm, δ(>N$CH_2CH_2$N<) = 1.89 ppm, δ(—$CH_2CH_2$CONH—) = 2.20 ppm, δ(—CHBr$CH_3$) = 4.07 ppm, δ(>N$CH_2CH_2$OCO—) = 3.80 ppm, δ(protons of —$CH_2CH_2$N< and —NH$CH_2CH_2$—) = 2.66–3.81 ppm.

### Synthesis of the star polymer PAMAM-*g*-PSt with polystyrene (PSt) arms grafted onto the surface of a PAMAM core

CuCl (0.04 g, 4 × $10^{-4}$ mol), HMTETA (0.092 g, 4 × $10^{-4}$ mol), St (6 mL, 0.05 mol), PAMAM–Br of generation 2 (0.107 g, 2.5 × $10^{-5}$ mol), and DMF (4 mL) were successively added to a flask. The mixture in the flask was degassed by three freeze–vacuum–thaw cycles. The flask was sealed *in vacuo* and then was immersed into an oil bath thermostated at 110°C under sufficient stirring. After the reaction was carried out for 12 h, the flask was rapidly cooled to room temperature by an ice bath. The polymer solution in tetrahydrofuran (THF) was passed through a short column of neutral alumina to remove the catalyst. The solution was concentrated under reduced pressure, and the crude polymer was precipitated in methanol. The product was dried in a vacuum oven at room temperature for further characterization. The route for the synthesis of PAMAM-*g*-PSt with PSt arms grafted onto the surface of the PAMAM core can be seen in Scheme 2.

IR (KBr): 2840 (s, $CH_2$), 2931 (as, $CH_2$), 3074 (C—H), 3028 (C—H), 1492 (C=C), 1608 $cm^{-1}$ (C=C).

### Micellization of the star polymer PAMAM-*g*-PSt

The self-assembled sample of PAMAM-PSt was prepared by the addition of 1 mg of polymers to 5 mL of a mixed solution of THF and methanol (1 : 4) at about 20°C. The prepared samples were blue and transparent, and this indicated the formation of aggregates.

### Characterization

Measurements of NMR spectra were conducted with a Bruker ARX-500 NMR spectrometer (Switzerland). Molecular weights and molecular weight distributions were measured on a Waters 410 gel permeation chromatography (GPC) apparatus (Beijing, China) equipped with a 10-μm Styragel HT6E column (300 mm × 7.8 mm) with linear PSt standards. THF was used as the eluent at a flow rate of 1 mL/min. The IR spectra of the polymers were recorded on a Nicolet Impact 410 at room temperature. The self-as-

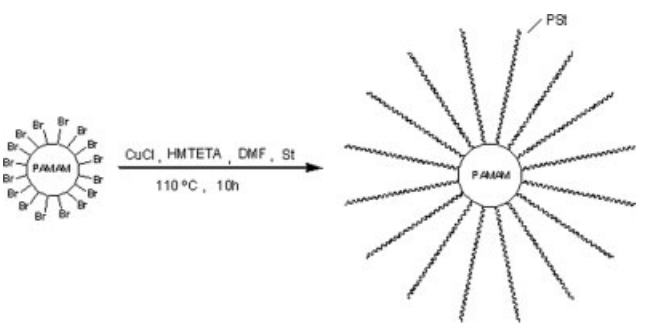


**Scheme 2** Route for the synthesis of PAMAM-*g*-PSt star polymers with PSt arms on the surface of a dendritic PAMAM core.

**TABLE II**
**Theoretical Properties of PAMAM Dendrimers, PAMAM–OH, and PAMAM–Br**

| Sample | Molecular formula | Molecular weight | Terminal group | Number of terminal groups |
|---|---|---|---|---|
| PAMAM G0.5 | $C_{18}H_{32}N_2O_8$ | 404 | $-COOCH_3$ | 4 |
| PAMAM G1.0 | $C_{22}H_{48}N_{10}O_4$ | 516 | $-NH_2$ | 4 |
| PAMAM G1.5 | $C_{54}H_{96}N_{10}O_{20}$ | 1204 | $-COOCH_3$ | 8 |
| PAMAM G2.0 | $C_{62}H_{128}N_{26}O_{12}$ | 1430 | $-NH_2$ | 8 |
| PAMAM–OH | $C_{94}H_{192}N_{26}O_{28}$ | 2134 | $-OH$ | 16 |
| PAMAM–Br | $C_{142}H_{240}Br_{16}N_{26}O_{44}$ | 4294 | $-OOCCH(CH_3)Br$ | 16 |

sembly of PAMAM-*g*-PSt star polymers was determined by atomic force microscopy (AFM) and scanning electron microscopy (SEM). AFM observations of the micelles absorbed onto the freshly treated silicon wafer surface were carried out with a commercial instrument (Multimode Nanoscope IIIa, Digital Instrument). All the tapping-mode images were taken at room temperature in air with microfabricated, rectangular crystal silicon cantilevers (Nanosensor). The topography images were obtained at a resonance frequency of approximately 365 kHz for the probe oscillation. The mean diameter and size distribution of the nanospheres were determined by the dynamic light scattering (DLS) method with a BI9000AT system from Brookheaven Instruments Corp.

## RESULTS AND DISCUSSION

### Synthesis of the dendritic macroinitiator PAMAM–Br

The synthesis of the dendritic macroinitiator includes the synthesis of PAMAM dendrimers, PAMAM–OH, and PAMAM–Br. The theoretical properties of PAMAM dendrimers, PAMAM–OH, and PAMAM–Br are listed in Table II.

The synthesis of PAMAM dendrimers includes a two-step interactive sequence, with the reported methods, to produce either ester- or amine-terminated structures. Iterative sequencing involves alkylation with methyl acrylate followed by amidation with excess ethylenediamine. The alkylation step produces ester-terminated subshells that are called half-generations. The second step involves amidation of the ester-terminated intermediates with a large excess of ethylenediamine to produce amine-terminated, full-generation dendrimers. In our studies, we used PAMAM dendrimers of the second generation (G2.0 PAMAM).

$^1$H-NMR spectra for sample PAMAM dendrimers with generations 0.5–2.0 are shown in Figure 1. The chemical shift of 3.69 ppm is attributed to protons originating from the COC$H_3$ segment [Fig. 1(1d,3i)]. As can be seen, no chemical shift for the COC$H_3$ segment of half-generation dendrimers appears in Figure 1(2,4). This is because methyl acrylate reacted with the full-generation dendrimers completely.

As reported previously, dendritic PAMAM–OH with multifunctional hydroxyl groups was first synthesized by PAMAM reacted with 2-chloroethanol in DMF, and nitrogen gas was removed in the HCl byproduct. Then, PAMAM–OH was acylated by 2-bromopropanoyl bromide to obtain PAMAM–Br, which could act as a macroinitiator for ATRP. After synthesis of the ATRP macroinitiator, the surface of PAMAM changed back to α-bromoester, and the formation of the macroinitiator was monitored with Fourier transform infrared (FTIR; Table I). Surface hydroxylation of PAMAM led to an increase in the characteristic hydroxyl band at 3350 cm$^{-1}$. After the introduction of the initiator functionality, the bands at 1740 and 1200 cm$^{-1}$, corresponding to the stretching vibrations of the C=O group and C—O, appeared. Meanwhile, the characteristic α-bromoester stretch at 669 cm$^{-1}$ appeared in the macroinitiator. The results indicated the formation of the α-bromoester groups in the terminal of PAMAM dendrimers and the disappearance of hydroxyl groups.

It was also confirmed by $^1$H-NMR that the PAMAM–OH surface was acylated by 2-bromopropanoyl bromide to yield PAMAM–Br (Fig. 2). In the $^1$H-NMR spectra, peaks assignable to the —CHBrC$H_3$ groups at 1.22 ppm and —C*H*BrCH$_3$ groups at 4.07 ppm were observed, whereas those due to the protons of PAMAM could still be seen clearly at 2.19–3.71 ppm. Thus, it can be concluded that under these conditions, PAMAM–Br can be successfully synthesized; that is, the hydroxyl groups are removed quantitatively, whereas the α-bromoester are connected to the terminal of the PAMAM dendrimers.

### Synthesis and characterization of the star polymer PAMAM-*g*-PSt

The synthetic procedure for star polymers is outlined in Scheme 2. With PAMAM–Br as the initiator and CuCl/HMTETA as the catalyst, ATRP of St occurs, yielding PAMAM-*g*-PSt star polymers. A large number of initiating centers on the same molecules greatly increase the possibility of crosslinking by

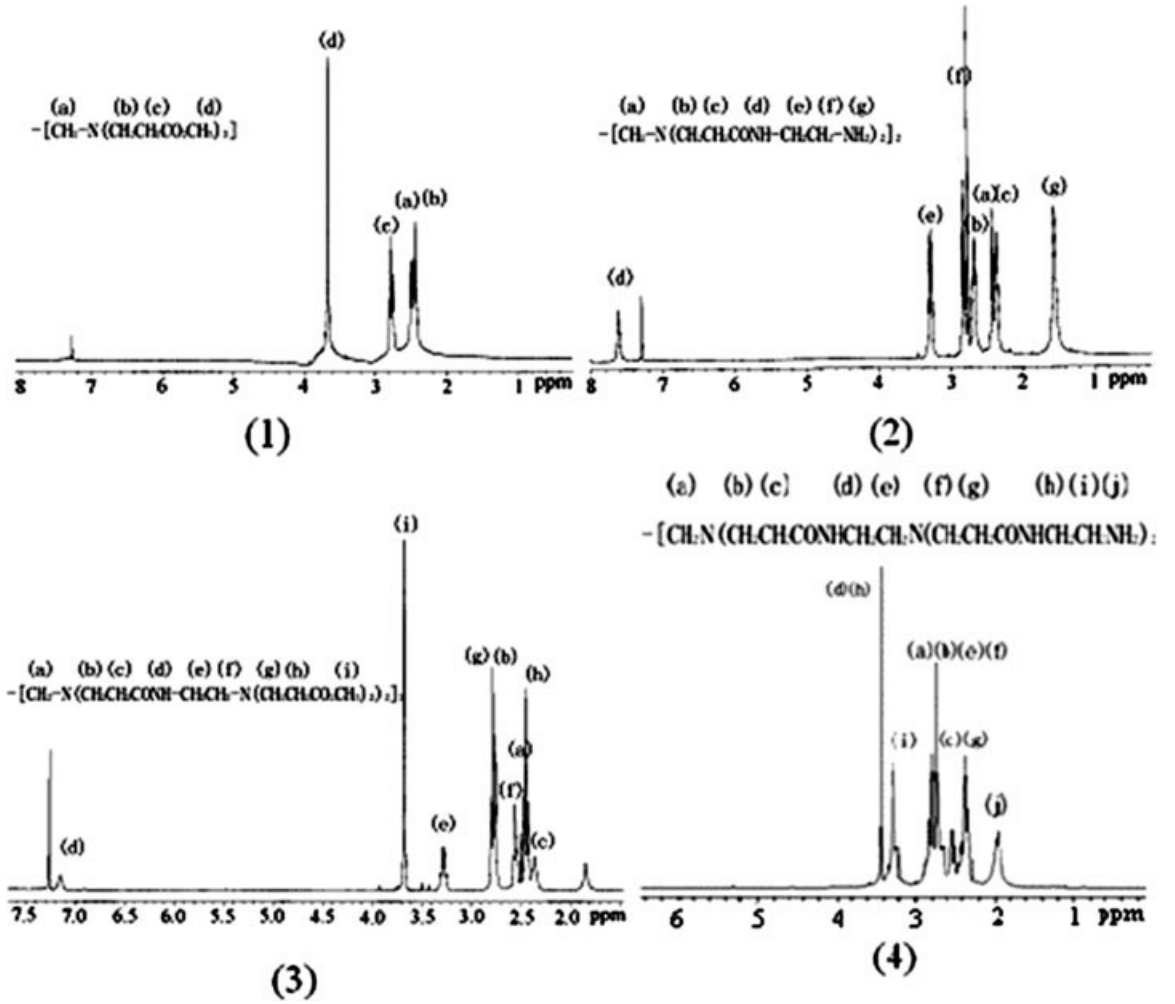


**Figure 1** $^{1}$H-NMR spectra of PAMAM: (1) G0.5, (2) G1.0, (3) G1.5, and (4) G2.0.

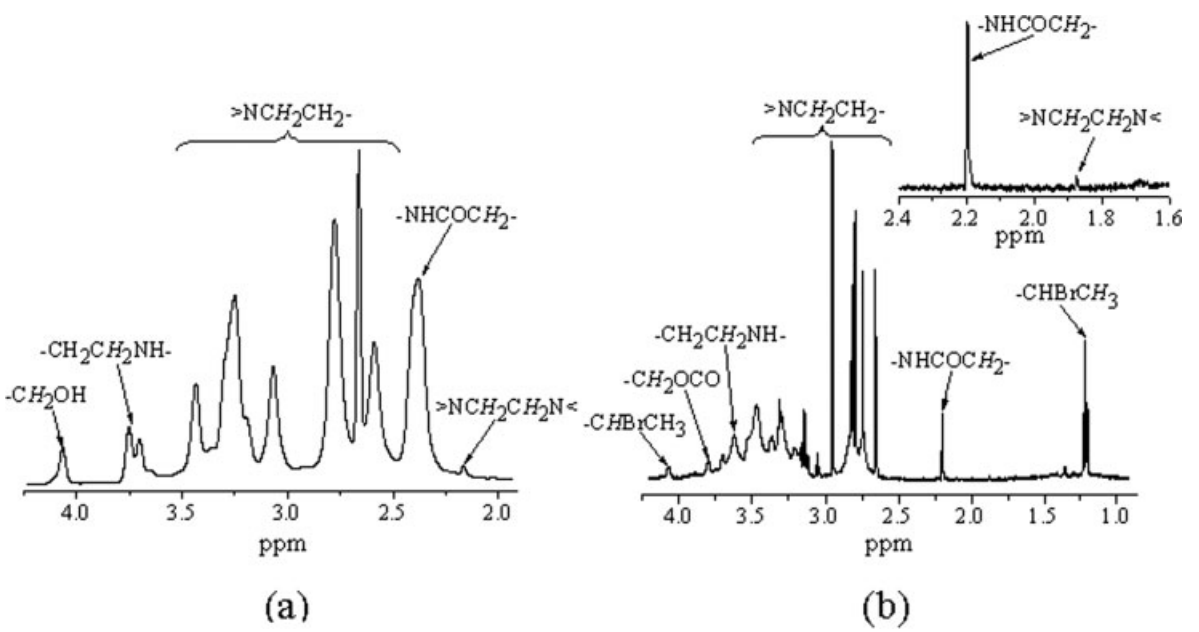


**Figure 2** $^{1}$H-NMR spectra of (a) PAMAM–OH and (b) PAMAM–Br.

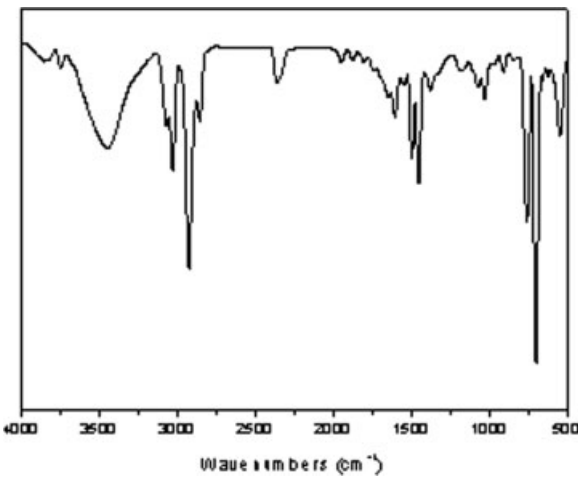


**Figure 3** IR spectrum of novel star polymer PAMAM-*g*-PSt.

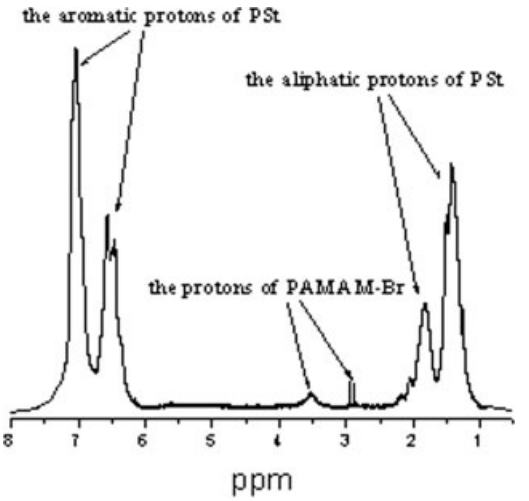


**Figure 4** $^1$H-NMR spectrum of PAMAM-*g*-PSt with generation 2.

coupling side reactions of the numerous growing radical chain ends. In our case, the dendritic core PAMAM–Br was used to initiate the polymerization, and no insoluble crosslinked materials were found. However, it is estimated that the coupling reactions of the growing radical chain ends could still exist to some extent to form the soluble coupling products.[36]

The characterization of the novel star polymers was investigated with FTIR and $^1$H-NMR. The detailed FTIR spectrum for PAMAM-*g*-PSt-based PAMAM with generation 2 is shown in Figure 3. The characteristic absorption peaks, occurring between 2844 and 2925 $cm^{-1}$, are associated with the symmetric and asymmetric C—H stretching vibrations of the aliphatic $CH_2$ groups. Other bands, including the C—H stretching vibration at 3074 and 3028 $cm^{-1}$ and C=C stretching vibration at 1492 and 1608 $cm^{-1}$, are characteristic of the segment of PSt. The peak at 3440 $cm^{-1}$ can be attributed to the stretching vibration of N—H, indicating the existence of the dendritic PAMAM unit. In the spectrum of PAMAM-*g*-PSt, another characteristic band at 1655 $cm^{-1}$ is assigned to the vibration of the amide group in PAMAM. However, the intensity of the band at 1655 $cm^{-1}$ obviously decreases.

The structure of PAMAM-*g*-PSt-based G2.0 PAMAM can be determined from the detailed $^1$H-NMR spectrum (Fig. 4). The peak assignable to the aromatic protons was observed at 7.03 and 6.56 ppm, indicating St units originating from the PSt segment. The smaller peak at 2.86–3.54 ppm is attributable to the protons of the macroinitiator, but the intensity of the peaks was lower in the $^1$H-NMR spectrum. The number of protons of the dendrimer core is 240, and the number of protons issued from St for the designed molecular weight of 244,200 is about 19,200, so the core represents only 1.25% of the total number of protons; it is difficult to ascertain the structure with such a ratio. The molecular weight determined from the $^1$H-NMR spectrum by integration of the protons of the PSt segment and the protons from the macroinitiator cannot be accurately calculated.

To obtain different degrees of polymerization, the reaction time was varied. As shown in Table III, the number-average molecular weight (or weight-average molecular weight) of star polymer PAMAM-*g*-PSt increases with the extension of the reaction time. However, the molecular weight of star polymers obtained by GPC are not authentic; the reason for this phenomenon is that GPC measurements based on a linear PSt standard underestimate the molecular weight of star macromolecules because of their different hydrodynamic volumes in comparison with linear PSt having the same molecular weight. The structure of star polymers complicates the determination of the molecular weights of the materials. Therefore, molecular weights obtained by GPC measurements should be used for comparison only.

From GPC analysis, the polydispersity of multiarm star polymers was around 2.0 (Table III). The possible

**TABLE III**
**Characteristics of PAMAM-*g*-PSt Star Polymers**

| | | GPC[a] | | |
|---|---|---|---|---|
| Sample | Time (h) | $M_n$ | $M_w$ | PDI |
| 1 | 2 | 148,100 | 373,800 | 2.52 |
| 2 | 3.5 | 177,700 | 393,000 | 2.21 |
| 3 | 5.5 | 195,500 | 409,900 | 2.09 |
| 4 | 8 | 201,000 | 407,300 | 2.02 |
| 5 | 11 | 221,900 | 435,000 | 1.96 |
| 6 | 15 | 222,100 | 431,100 | 1.94 |

$M_n$ = number-average molecular weight; $M_w$ = weight-average molecular weight; PDI = polydispersity index.
[a] Calibrated against linear PSt standards.

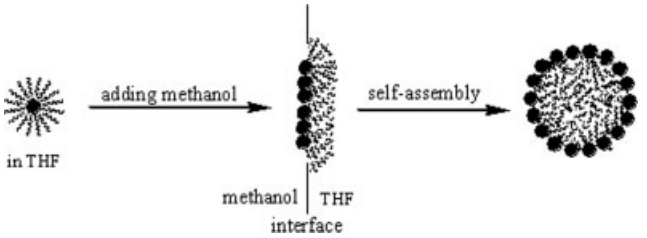


**Scheme 3** Formation of large multimolecular micelles by the secondary aggregation of unimolecular micelles.

reason for the broad distribution of molar masses could be incomplete substitution with $CHBrCH_3$ groups, which led to stars with different numbers of arms. The number of α-bromoesters groups could be lower than the average for lower molecular weight fractions and higher than the average for high-molecular-weight fractions. It could be deduced that the polydispersity index of star polymers was still broad after ATRP of St on the surface of PAMAM–Br.

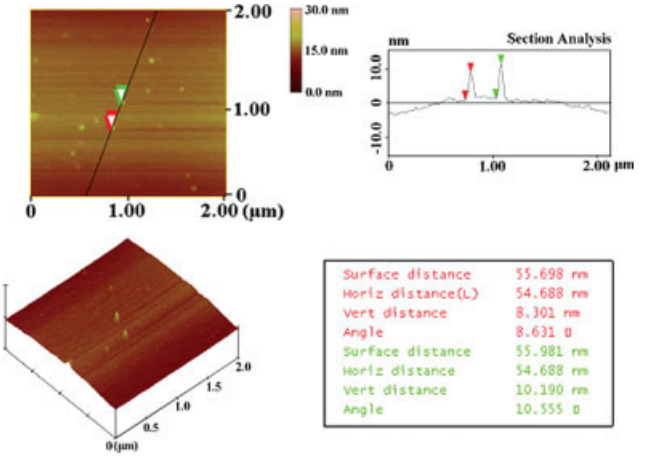


**Figure 5** AFM images of PAMAM-*g*-$PSt_{50}$ in the select solvent (THF/methanol) with a concentration of star polymers of 1 mg/mL and a volume ratio of 1 : 4. [Color figure can be viewed in the online issue, which is available at www.interscience.wiley.com.]

## Self-assembly properties of the star polymer PAMAM-*g*-PSt

It is well known that the different morphologies of self-assembly systems are basically related to the chemical compositions of the polymers and to the relative volume ratio of the two blocks. Among the possible morphologies, spherical micelles are of special interest because they have the lowest surface energies[37–39] and can lead to encapsulating active molecules such as DNA, enzymes, and drugs. The star polymers (PAMAM-*g*-PSt) consist of two segments: a dendritic core and many PSt arms. The arms can be dissolved in THF; however, methanol is a good solvent for a dendritic core. Therefore, it is assumed that the PAMAM cores are encapsulated in the aggregates and that excess PSt arms are hidden in the nanoparticles (Scheme 3).

To observe the self-assembly behaviors, the star polymers were treated as follows: sample 1, sample 2, and sample 3 with different molar ratios of St to the macroinitiator (as shown in Table IV) were separately dissolved in 1 mL of THF at room temperature and then dropped into 4 mL of methanol under stirring. After 10 min of stirring, a few drops of the mixtures were poured onto rectangular crystal silicon cantilevers. The samples were left at room temperature for 1 night before observation.

The morphologies of sample 1, sample 2, and sample 3 that formed from THF/methanol mixed solutions were directly observed by AFM. Self-assembly of the novel star polymers in THF/methanol (1 : 4 v/v) mixed solutions is shown in Figures 5–7. From the images, we can find that flat, spherical aggregates formed in these samples. The average diameters of the spherical nanoparticles were around 50 nm for sample 1, 90 nm for sample 2, and 140 nm for sample 3. From these phenomena, we concluded that the number of PSt arms plays an important role in controlling the size of self-assembly structures. When the phenyl units of PSt arms are stacked in a certain direction and have a short enough distance, p–p stacking interactions can be formed among them. Although the π–π interaction of phenyls is very weak, the p–p stacking interactions can also drive the molecular self-assembly process and strengthen the

**TABLE IV**
**Sizes of Different Novel PAMAM-*g*-PSt Nanospheres**

| Sample | $R_{S/M}$ | Yield (%) | $M_{th}$ | $R_h$ (nm) | | PDI by DLS at 25°C |
|---|---|---|---|---|---|---|
| | | | | AFM | DLS at 25°C | |
| 1 | 50 | 82 | 84,200 | ~ 50 | ~ 130 | 0.12 |
| 2 | 100 | 90 | 164,200 | ~ 90 | ~ 210 | 0.11 |
| 3 | 150 | 95 | 244,200 | ~ 140 | ~ 240 | 0.19 |

$M_{th}$ = theoretical weight; PDI = polydispersity index; $R_h$ = hydrodynamic diameter; $R_{S/M}$ = molar ratio of styrene to the macroinitiator.

[a]Yield = $[W_{PAMAM\text{-}g\text{-}PSt}/(W_{St} + W_{PAMAM\text{–}Br})] \times 100\%$, where $W_{PAMAM\text{-}g\text{-}PSt}$, $W_{St}$, and $W_{PAMAM\text{–}Br}$ are the weights of the star polymers, monomer (styrene), and macroinitiator (PAMAM–Br), respectively.

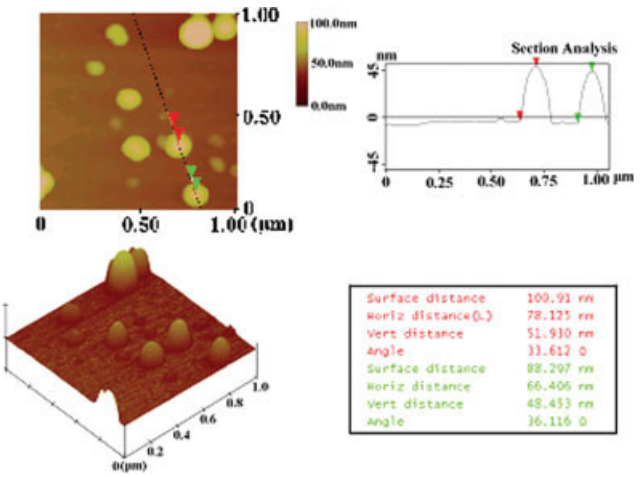


**Figure 6** AFM images of PAMAM-*g*-$PSt_{100}$ in the select solvent (THF/methanol) with a concentration of star polymers of 1 mg/mL and a volume ratio of 1 : 4. [Color figure can be viewed in the online issue, which is available at www.interscience.wiley.com.]

self-assembly structures[40,41] (Scheme 3). In the procedure of self-assembly, with p–p stacking interactions between the phenyl units, spherical structures are formed with the smallest surface energy.

DLS measurements gave further information on the size of the micelles. Table IV shows a typical size distribution of star polymer PAMAM-*g*-PSt micelles. The size distribution is broad. The broad micelle size distribution might be attributed to the formation of larger micellar clusters. Eisenberg and coworkers[42,43] reported that micelles in solutions can further aggregate to form large compound micelles. The hydrodynamic diameter values obtained from DLS studies are larger than those observed with AFM. The reason for this difference might be that the micelles were swollen in solutions during the DLS measurements, whereas AFM showed the diameter of the dried aggregates.

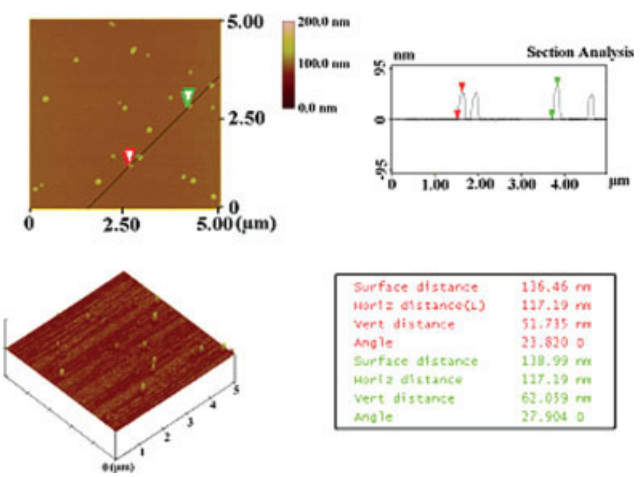


**Figure 7** AFM images of PAMAM-*g*-$PSt_{150}$ in the select solvent (THF/methanol) with a concentration of star polymers of 1 mg/mL and a volume ratio of 1 : 4. [Color figure can be viewed in the online issue, which is available at www.interscience.wiley.com.]

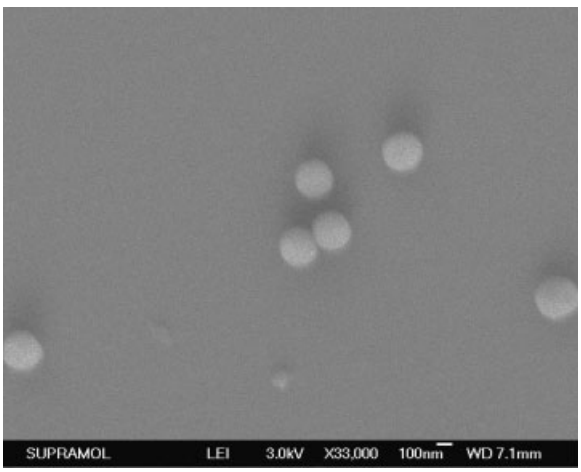


**Figure 8** Typical SEM image of micelles prepared from star polymer PAMAM-*g*-PSt with a molar ratio of St to the macroinitiator of 150.

SEM was also used to explore the morphology of the aggregates. Figure 8 shows a representative SEM image of the flat, spherical micelles prepared from sample 3. The spherical micelles looked smooth and regular. The average diameters of the micelles, determined by SEM, were 130–140 nm. This corresponded to the results of the AFM image.

## CONCLUSIONS

Novel PAMAM-*g*-PSt star polymers with PSt arms of different lengths were synthesized successfully by ATRP with a dendritic PAMAM–Br macroinitiator in the presence of CuCl and HMTETA as a catalyst system. The PAMAM–Br macroinitiator was obtained through a two-step chemical modification of the PAMAM dendrimer cores by substitution of the terminal amine groups with 2-chloroethanol to obtain PAMAM–OH, which had hydroxyl groups in the terminal, and then the terminal hydroxyl groups were substituted with 2-bromopropanoyl bromide with TEA as an acceptor of HBr. The structures of the polymers were confirmed with FTIR, $^1$H-NMR, and GPC. A detailed microstructural analysis of the structure revealed that self-assembled structures could be formed in selected solvents (THF/methanol). Here we report the self-assembly of large multimolecular micelles from a series of newly synthesized star polymers. The micellization behavior was investigated with AFM, SEM, and DLS. The results demonstrate that these large micelles are multimicelle aggregates formed by the secondary aggregation of unimolecular micelles. The self-

assembly mechanism presented here may be extended to the micellar self-assembly of other dendritic polymers, especially large micelles.

## References


1. Hadjichristidis, N.; Pitsikalis, M.; Pispas, S.; Iatrou, H. Chem Rev 2001, 101, 3747.
2. Liu, H.; Xu, J.; Jiang, J.; Yin, J.; Narain, R.; Cai, Y.; Liu, S. J Polym Sci Part A: Polym Chem 2007, 45, 1446.
3. Jia, Z.; Zhou, Y.; Yan, D. J Polym Sci Part A: Polym Chem 2005, 43, 6534.
4. Lee, H. J.; Lee, K.; Choi, N. J Polym Sci Part A: Polym Chem 2005, 43, 870.
5. Zhang, X.; Xia, J.; Matyjaszewski, K. Macromolecules 2000, 33, 2340.
6. Baek, K. Y.; Kamigaito, M.; Sawamoto, M. J Polym Sci Part A: Polym Chem 2002, 40, 2245.
7. Baek, K. Y.; Kamigaito, M.; Sawamoto, M. J Polym Sci Part A: Polym Chem 2002, 40, 1972.
8. Bosman, A. W.; Vestberg, R.; Heumann, A.; Frechet, J. M. J.; Hawker, C. J. J Am Chem Soc 2003, 125, 715.
9. Baek, K. Y.; Kamigaito, M.; Sawamoto, M. J Polym Sci Part A: Polym Chem 2002, 40, 633.
10. Hou, S.; Chaikof, E. L.; Taton, D.; Gnanou, Y. Macromolecules 2003, 36, 3874.
11. Lu, J.; Zhang, X.; Zhao, S.; Yang, W. J Appl Polym Sci 2007, 104, 3917.
12. Stenzel, M. H.; Davis, T. P. J Polym Sci Part A: Polym Chem 2002, 40, 4498.
13. Moschogianni, P.; Pispas, S.; Hadjichristidis, N. J Polym Sci Part A: Polym Chem 2001, 39, 650.
14. Knischka, R.; Lutz, P. J.; Sunder, A.; Mulhaupt, R.; Frey, H. Macromolecules 2000, 33, 315.
15. Hao, X.; Nilsson, C.; Jesberger, M.; Stenzel, M. H.; Malmström, E.; Davis, T.; Östmark, P. E.; Barner-Kowollik, C. J Polym Sci Part A: Polym Chem 2004, 42, 5877.
16. Hou, J.; Yan, D. Macromol Rapid Commun 2002, 23, 456.
17. Zhao, Y. L.; Cai, Q.; Jing, J.; Shuai, X. T.; Bei, J. Z.; Chen, C. F.; Xi, F. Polymer 2002, 43, 5819.
18. Heise, A.; Diamanti, S.; Hedrick, J. L.; Frank, C. W.; Miller, R. D. Macromolecules 2001, 34, 3798.
19. Taton, D.; Gnanou, Y.; Matmour, R.; Angot, S.; Hou, S.; Francis, R.; Lepoittevin, B.; Moinard, D.; Babin, J. Polym Int 2006, 55, 1138.
20. Bucknall, D. G.; Anderson, H. L. Science 2003, 302, 1904.
21. Antonietti, M.; Förster, S. Adv Mater 2003, 15, 1323.
22. Discher, D. E.; Eisenberg, A. Science 2002, 297, 967.
23. Discher, B. M.; Won, Y. Y.; Ege, D.; Lee, J. C. M.; Bates, F. S.; Discher, D. E.; Hammer, D. A. Science 1999, 284, 1143.
24. Yan, D. Y.; Zhou, Y. F.; Hou, J. Science 2004, 303, 65.
25. Zhou, Y.; Yan, D. Angew Chem Int Ed 2004, 43, 4896.
26. Zhang, L.; Eisenberg, A. Science 1995, 268, 1728.
27. Zhang, L.; Yu, K.; Eisenberg, A. Science 1996, 272, 1777.
28. Terreau, O.; Bartels, C.; Eisenberg, A. Langmuir 2004, 20, 637.
29. Cameron, N. S.; Eisenberg, A.; Brown, G. R. Biomacromolecules 2002, 3, 124.
30. Zhang, L.; Eisenberg, A. J Am Chem Soc 1996, 118, 3168.
31. Yu, K.; Eisenberg, A. Macromolecules 1996, 29, 6359.
32. Keller, R. N.; Wrcoff, H. D.; Marchi, L. E. Inorg Synth 1946, 2, 1.
33. Tomalia, D. A.; Baker, H.; Dewald, J. R.; Hall, M.; Kallos, G.; Martin, S. Polym J 1985, 17, 117.
34. Wang, J.; Jia, X.; Zhong, H.; Wu, H.; Li, Y.; Xu, X.; Li, M.; Wei, Y. J Polym Sci Part A: Polym Chem 2000, 38, 4147.
35. Hu, H.; Fan, X.; Cao, Z. Polymer 2005, 46, 9514.
36. Yan, D.; Hou, J.; Zhu, X.; Kosman, J. J.; Wu, H. S. Macromol Rapid Commun 2000, 21, 557.
37. Zhang, L.; Wan, M. Adv Funct Mater 2003, 13, 815.
38. Malmstroem, E.; Johansson, M.; Hult, A. Macromolecules 1995, 28, 1698.
39. Zhai, X.; Peleshanko, S.; Klimenko, N. S.; Genson, K. L.; Vaknin, D.; Shevchenko, V. V.; Tsukruk, V. V.; Vortman, M. Y.; Zhao, Y.; Song, Y.; Jiang, W.; Zhang, B.; Li, Y.; Sha, K.; Wang, S.; Chen, L.; Ma, L.; Wang, J. Macromolecules 2003, 36, 3101.
40. (a) Jiang, G.; Wang, L.; Chen, T.; Yu, H.; Wang, C.; Chen, C. Polymer 2005, 46, 5351; (b) Sun, J.; Tang, H.; Jiang, J.; Xie, P.; Zhang, R.; Fu, P. F.; Wu, Q. Polymer 2003, 44, 2867.
41. Zhang, L.; Eisenberg, A. Science 1995, 268, 1728.
42. Zhang, L.; Eisenberg, A. J Am Chem Soc 1996, 118, 3168.
43. Yu, K.; Zhang, L.; Eisenberg, A. Langmuir 1996, 12, 5980.